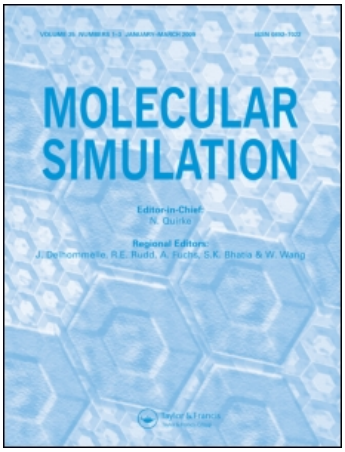

Molecular Simulation
Publication details, including instructions for authors and subscription information:
http://www.informaworld.com/smpp/title~content=t713644482

The Rheology of Liquid Pentane Isomers by Non-Equilibrium Molecular Dynamics Simulations

Song Hi Lee[a]
[a] Department of Chemistry, Kyungsung University, Pusan, Korea

To cite this Article Lee, Song Hi(2000) 'The Rheology of Liquid Pentane Isomers by Non-Equilibrium Molecular Dynamics Simulations', Molecular Simulation, 23: 4, 243 — 256
To link to this Article: DOI: 10.1080/08927020008025371
URL: http://dx.doi.org/10.1080/08927020008025371

Molecular Simulation, 2000, Vol. 23, pp. 243–256
Reprints available directly from the publisher
Photocopying permitted by license only

THE RHEOLOGY OF LIQUID PENTANE ISOMERS BY NON-EQUILIBRIUM MOLECULAR DYNAMICS SIMULATIONS

SONG HI LEE

Department of Chemistry, Kyungsung University, Pusan, Korea 608-736

(Received August 1999; accepted August 1999)

In this paper, non-equilibrium molecular dynamics (NEMD) simulations of planar Couette flow are reported for an expanded collapsed atom model for liquid pentane isomers at 273.15 K. The strain rate dependent viscosity for liquid pentane isomers exhibits shear-thinning and a linear dependence on $\gamma^{1/2}$. Newtonian viscosities for liquid pentane isomers obtained by a linear extrapolation to zero strain rate are: 0.256 cP for normal pentane, 0.219 cP for isopentane, and 0.168 cP for neopentane. The strain rate dependent pressure difference and normal stress difference vary nearly linearly with the $\gamma^{3/2}$ law and the γ law, respectively, for all three liquid pentane isomers. The overall trend of the square of radius of gyration and end-to-end distance for normal pentane is a linear increase with strain rate. For isopentane, the trend hardly changes for the range of shear rate in this study. The alignment angle decreases with increasing strain rate and the alignment angle of the straight chain alkane is less than that of the branched chain alkane. The average percentage of C—C—C—C *trans* for normal pentane as a function of strain rate is in excellent correlation with the square of the radius of gyration and the average end-to-end distance. Applying the strain rate in the x-direction, the alignment angle is forced to decrease and the percentage of C—C—C—C *trans* increases with increasing strain rate.

Keywords: Pentane; rheology; NEMD

I. INTRODUCTION

Normal pentane is an example of a straight chain alkane. Each carbon atom within the chain is bonded to no more than two other carbon atoms and unbranched alkanes contain only primary and secondary carbon atoms. Isopentane and neopentane are examples of branched chain alkanes. In neopentane the central carbon atom is bonded to four carbon atoms. Normal pentane, isopentane and neopentane have the same molecular formula: C_5H_{12}. The atoms of the three compounds connected in a different

order and are, therefore, constitutional isomers [1]. These three different geometries of pentane isomers are shown in Figure 1.

Constitutional isomers, which have the same carbon number but different structures, have different physical properties. They are found to have different melting points, boiling points, densities, indexes of refraction, and so forth, although they may not be large. For example, a branched chain isomer has a lower boiling point than a straight chain isomer. Thus, normal pentane has a boiling point of 36°C, isopentane with a single branch 28°C, and neopentane with two branches 9.5°C. The effect of branching on boiling point is observed within all families of organic compounds. It is reasonable that branching should lower the boiling point: with branching the molecular shape tends to approach that of a sphere, and as this happens the surface area decreases, with the result that the intermolecular forces become weaker and are overcomed at a lower temperature.

The branching effect on the dynamic properties of liquid alkanes, such as self diffusion coefficient, viscosity, and thermal conductivity, is one of the most interesting phenomena. For liquid butane, the experimentally observed behavior [2] tells us that viscosity increases with branching. For liquid pentane, hexane, and heptane, however, branching decreases the viscosity, for example, 0.289 and 0.273 cP at 273.15 K, and 0.240 and 0.223 cP at 293.15 K for normal pentane and isopentane, 0.326 and 0.306 cP at 293.15 K for

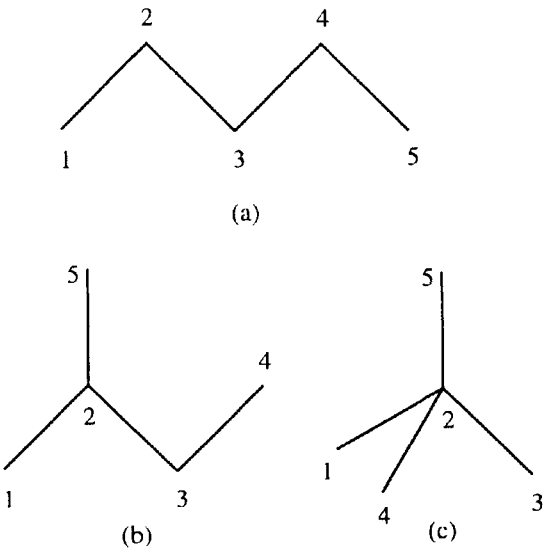

FIGURE 1 Geometries of (a) normal pentane, (b) isopentane, and (c) neopentane.

normal hexane and isohexane, and 0.409 and 0.384 cP at 293.15 K for normal heptane and isoheptane [3], respectively. These experimental results, except for liquid butane, indicate that as the molecular shape tends to approach that of a sphere and the surface area tends to decrease with branching, the intermolecular forces become weaker and the viscosity of alkane isomers decreases.

In the present paper, we examine the Newtonian and strain rate dependent rheological properties of liquid pentane isomers – normal pentane, isopentane, and neopentane – by performing non-equilibrium molecular dynamics(NEMD) simulations for an collapsed atomic model at 273.15 K. The main goal here is to investigate the branching effect on the rheological properties of liquid pentane isomers. The number of branches is different for each of the three C_5 alkanes with the same molecular formula: C_5H_{12}. Are the subtle differences in branching reflected in differences in their rheological properties?

In Section II we present the molecular models and MD simulation method. We discuss our simulation results in Section III and present the concluding remarks in Section IV.

II. MOLECULAR MODELS AND MOLECULAR DYNAMICS SIMULATIONS

The expanded collapsed atomic model [4–6] includes the C—C bond stretching and C—C—C bond angle bending potential in addition to the Lennard-Jones (LJ) and torsional rotational potentials of the original Rykaert-Bellemans' (RB) collapsed atomic model [7]:

$$V_b(r_{ij}) = K_0(r_{ij} - r_e)^2 \tag{1}$$

$$V_a = K_1(\theta - \theta_e)^2 - K_2(\theta - \theta_e)^3 \tag{2}$$

The equilibrium bond length (r_e) is fixed at 1.53 Å, and the bond angles (θ_e) are also fixed at 109.47 degrees. The force constants (K_0, K_1, and K_2) are used by Lee *et al.* [8–13] and Chynoweth *et al.* [4–6], which are originally provided by the work of White and Boville [14], and are given in Table I.

In the original RB model [7], monomeric units are treated as single spheres with the masses given in Table II. They interact through an LJ potential between the spheres in different molecules and between the spheres

TABLE I Potential parameters of the expanded collapsed atom model

LJ parameters	σ (nm)	ε (KJ/mol)				
	0.3923	0.5986				
torsional	co (KJ/mol)	c_1	c_2	c_3	c_4	c_5
C—C—C—C	9.279	12.136	−13.120	−3.060	26.240	−31.495
bond stretching	r_e (nm)	K_0 (kJ/mol nm^2)				
C—C	0.153	132600				
Bond angle bending	θ_e (deg)	K_1 (kJ/mol deg^2)			K_2 (kJ/mol deg^3)	
C—C—C—	109.47	0.05021			0.000482	

TABLE II Molecular dynamics simulation parameters of the expanded collapsed atom model for liquid pentane isomers

Pentane isomers	*Number of molecules*	*Mass of site (g/mole)*	*Temperature (K)*	*Density (g/cc)*	*Length of box (nm)*
n-pen	64	14.42996	273.15	0.645	2.2823
i-pen	64	14.42996	273.15	0.639	2.2894
neo-pen	64	14.42996	273.15	0.613	2.3213

more than three places apart on the same molecule. The C—C—C—C torsional rotational potential is given as

$$V(\phi) = c_0 + c_1\cos\phi + c_2\cos^2\phi + c_3\cos^3\phi + c_4\cos^4\phi + c_5\cos^5\phi \qquad (3)$$

where ϕ is the C—C—C—C dihedral angle. The Lennard-Jones parameters and c_i's are listed in Table I. Unlike in normal pentane, there are multiply imposed torsional rotational potentials in isopentane. That is to say, one doubly imposed dihedral state on the bond of C_2—C_3 in isopentane exists, as shown in Figure 1.

In an equilibrium molecular dynamics(EMD) simulation, the Green-Kubo relation for the shear viscosity, η, is given by the integral of the stress auto-correlation function:

$$\eta = \frac{V}{kT}\int_0^\infty \langle P_{xy}(0)P_{xy}(t)\rangle dt, \qquad (4)$$

where P_{xy} is an off-diagonal ($x \neq y$) of the viscous pressure tensor. The pressure tensor **P** is expressed in terms of molecular quantities by

$$\mathbf{P}V = \sum_{\mathbf{i}=1}^{N} \frac{\mathbf{p_i p_i}}{M} + \sum_{1\leq \mathbf{i}} \sum_{\leq \mathbf{j} < N} \mathbf{r_{ij} F_{ij}}, \qquad (5)$$

where V is the volume of the system, $\mathbf{r}_{ij} = \mathbf{r}_i - \mathbf{r}_j$ is the vector joining the centers of molecules i and j, $\mathbf{F}_{ij}$ is the force between them. The alternative method proposed by Evans [15] and derived using the principles of linear-irreversible thermodynamics [16, 17] takes advantage of the isotropic symmetry but makes use of the full pressure tensor, which allows for improved statistics:

$$\eta = \frac{V}{10kT}\int_0^\infty \langle Tr[\tilde{P}(0)\tilde{P}(t)]\rangle dt, \tag{6}$$

where $\tilde{P}$ is symmetric traceless part of the full pressure tensor.

For the study of planar Couette flow, in which fluids are subjected to homogeneous shear between two parallel plates, the NEMD algorithm for alkane is a molecular version of the SLLOD algorithm [18, 19]. The equations of motion for site s in molecule i are given by

$$\frac{d\mathbf{r}_{is}}{dt} = \frac{\mathbf{p}_{is}}{m_s} + \mathbf{n}_x \gamma y_i \tag{7}$$

and

$$\frac{d\mathbf{p}_{is}}{dt} = \mathbf{F}_{is} - \mathbf{n}_x \frac{m_s}{M}\gamma p_{yi} - \alpha \frac{m_s}{M}\mathbf{p}_i, \tag{8}$$

where $M = \sum_s M_s$, $\mathbf{r}_i = \sum_s (m_s/M)\mathbf{r}_{is}$, and $\mathbf{F}_i = \sum_s \mathbf{F}_{is}\cdot\mathbf{n}_x$ is the unit vector in the x-direction, $\mathbf{F}_{is}$ is the force exerted by the other sites in the same and different molecules on the site s in molecule i, γ is the strain rate, $\partial u_x/\partial y$, and α is the thermostatting constant, given by

$$\alpha = \frac{\sum_{i=1}^N [\mathbf{F}_i \cdot \mathbf{p}_i - \gamma p_{yi} p_{xi}]}{\sum_{i=1}^N p_i^2} \tag{9}$$

The effect of the thermostatting term involving $\gamma(m_s/M)\mathbf{p}_i$ in Eq. (7) is to hold the translational center-of-mass kinetic energy constant. The momenta in Eqs. (6) and (7) are measured with respect to the streaming velocity of the fluid and are known as peculiar momenta.

These equations of motion are combined with the Lees-Edwards "sliding brick" boundary conditions [20]. In the absence of the thermostat, the terms in Eqs. (7) and (8) involving the strain field, γ, cancel to yield Newton's equations of motion relating $\mathbf{r}_i$ and $\mathbf{F}_i$. This implies that the SLLOD algorithm truly generates boundary driven planar Couette flow, leading to the conclusion that it is correct to arbitrarily order the strain rate when

appropriately thermostatted [21]. The strain rate dependent shear viscosity is then obtained from Newton's law of viscosity

$$\eta = -\frac{P_{xy} + P_{yx}}{2\gamma}, \tag{10}$$

where P_{xy} and P_{yx} are the averaged xy and yx components of P.

The molecular dynamics simulation parameters such as number of molecules, mass of site, temperature, and length of simulation box are listed in Table II. The density of isopentane at 273.15 K was not found in the literature of chemistry, thus it was inferred from the density values at other temperatures, namely 0.62473 at 288.15 K, 0.61972 at 293.15 K, and 0.61455 at 298.15 K. A canonical ensemble of fixed $N(= 64$ molecules), V (length of cubic box), and $T(= 273.15\,\text{K})$ was chosen for the simulation ensemble. Gauss's principle of least constraint [22, 23] was used to maintain the system at a constant temperature according to Eqs. (8) and (9). A spherical cut-off of radius $R_c = 2.5\,\sigma$, where σ is the LJ parameter, was employed for all the pair interactions. For the integration over time, we adopted Gear's fifth-order predictor-corrector algorithm [24] with a time step of 0.0005 ps. More than 1,000,000 time steps were simulated for the average and the configurations of molecules were stored every 10 time steps for further analysis.

III. RESULTS AND DISCUSSION

In Figure 2, the strain rate dependent viscosities of the expanded collapsed atom model for liquid pentane isomers at 273.15 K are plotted. Detailed numerical data and production run lengths are tabulated in Table III with the calculated pressures. The calculated viscosities for liquid pentane isomers show shear-thinning over the range of strain rate in this study and the dependence of the calculated viscosities on $\gamma^{1/2}$ appear almost linear. The Newtonian viscosities for liquid pentane isomers obtained by a linear extrapolation to zero strain rate from our NEMD simulations at 273.15 K are: 0.256 cP for normal pentane, 0.219 cP for isopentane, and 0.168 cP for neopentane. The experimental viscosity of normal pentane at temperature 273.15 K is 0.289 cP and that of isopentane is 0.273 cP. The agreement between the calculated shear viscosities and the experimental values is generally acceptable for the two pentane isomers at 273.15 K. The equilibrium molecular dynamics(EMD) results for the viscosity of liquid pentane isomers at 273.15 K [25] calculated from the Green-Kubo relation also give

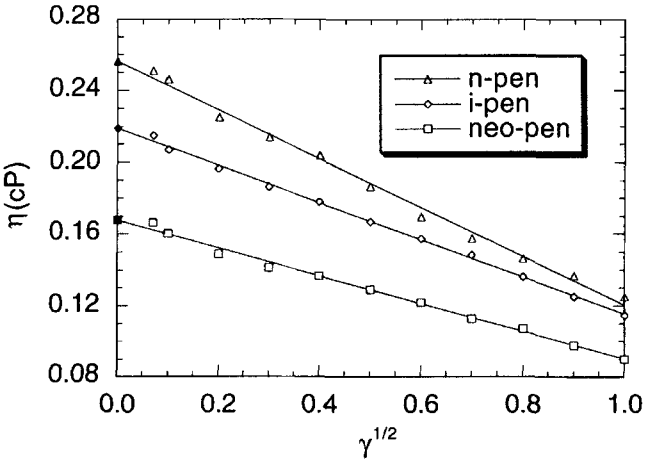

FIGURE 2 The strain rate dependent viscosity (cP) for liquid pentane isomers at 273.15 K. Black symbols are obtained by extrapolating to zero strain rate.

TABLE III The viscosity and pressure of the expanded collapsed atom model for pentane isomers at various strain rates obtained from our NEMD simulations at 273.15 K (numbers in the parentheses represent the statistical uncertainty in the least significant digits)

Run		*n-pen*		*i-pen*		*neo-pen*	
length(ns)	$\gamma(ps^{-1})$	$\eta(cP)$	*P(bar)*	$\eta(cP)$	*P(bar)*	$\eta(cP)$	*P(bar)*
2.4	0.005	0.251(131)	268(10)	0.215(110)	71(9)	0.166(94)	−146(9)
2.0	0.01	0.246(78)	270(8)	0.207(76)	72(8)	0.160(62)	−145(10)
1.8	0.04	0.225(17)	273(11)	0.196(15)	74(10)	0.149(12)	−144(12)
1.8	0.09	0.214(10)	279(14)	0.186(7)	85(7)	0.141(8)	−142(7)
1.8	0.16	0.204(8)	303(7)	0.178(7)	99(5)	0.137(6)	−122(9)
1.5	0.25	0.186(7)	336(7)	0.167(6)	131(11)	0.129(7)	−106(10)
1.5	0.36	0.169(7)	392(6)	0.157(8)	181(5)	0.122(4)	−74(4)
1.5	0.49	0.157(6)	471(8)	0.148(5)	251(6)	0.113(4)	−31(6)
1.2	0.64	0.146(4)	574(8)	0.136(5)	375(14)	0.107(3)	25(6)
1.2	0.81	0.137(3)	710(7)	0.125(2)	465(11)	0.098(2)	98(5)
1.2	1.00	0.125(3)	906(8)	0.114(2)	637(10)	0.090(2)	213(14)

a quite acceptable agreement(0.267, 0.245, and 0.150 cP) with the present NEMD results. As the molecular shape tends to approach that of a sphere and the surface area tends to decrease with branching, the viscosity of liquid pentane isomers decreases.

There are various methods for extrapolating to zero strain rate to obtain the Newtonian viscosity [6]. From kinetic and mode coupling theories [26–28], it is known that for simple atomic fluids [29–31] and small chain molecules [4, 8–9, 32–37], the strain rate dependence of the shear viscosity is linear in $\gamma^{1/2}$. To apply the SLLOD algorithm to a Newtonian

fluid, it is necessary to perform several simulations at different strain rates γ and fit the resulting strain rate dependent viscosities to the equation

$$\eta = \eta_0 + \eta_1 \gamma^{1/2}, \tag{11}$$

where the zero strain rate extrapolation of η, η_0, is thus the Newtonian viscosity. For liquid alkanes, the power law behavior of the viscosity *vs.* strain rate indicates a qualitative difference between the dynamical behaviors of the long-chain alkanes and small chain molecules [38] and a further difference between those of the straight-chain and the branched-chain alkanes [10].

We show in Figure 3 the strain rate dependent pressure difference of the expanded collapsed atom model for liquid pentane isomers at 273.15 K. Detailed numerical data and production run lengths are tabulated in Table III. The equilibrium pressure at zero strain rate is negative for neopentane. At low strain rate, the pressure is nearly equal to the equilibrium pressure, and at relatively high strain rate, the pressure increases nearly linearly with the two-thirds power of the strain rate. For simple atomic liquids, both mode coupling theory and simulations suggest that the pressure, p, and the configuration energy, E_{conf}, satisfy the asymptotic relations

$$p = p_0 + p_1 \gamma^{3/2} \quad \text{and} \quad E_{\text{conf}} = E_0 + E_1 \gamma^{3/2}. \tag{12}$$

Figure 3 shows that for the range of shear rate studied in this work, the $\gamma^{3/2}$ power law describes the results very well for all liquid pentane isomers at

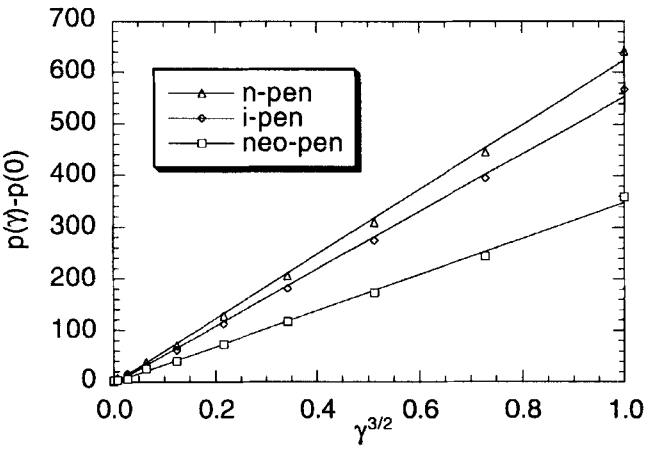

FIGURE 3 The strain rate dependent pressure difference(atm) of the expanded collapsed atom model for liquid pentane isomers at 273.15 K (1 atm = 1.01325 bar = 0.101325 MPa).

273.15 K. Another good example of the $\gamma^{3/2}$ power law description of shear dilatancy is that of normal decane by NEMD [37]. In an earlier NEMD study, however, of 6-propyl duodecane and 5-dibutyl nonane [10], the shear dilatancy does not show significant dependence on strain rate because of the complexity of the chain molecules. Recent computer simulations have produced a variety of behaviors for shear dilatancy of hydrocarbon chain liquids [34, 39].

The strain rate dependent normal stress difference of the expanded collapsed atom model for liquid pentane isomers at 273.15 K is plotted in Figure 4. Bird *et al.* [40] have devised a convenient representation of normal stress effects by defining the material functions ψ_1 and ψ_2, which are related to normal stress differences by $\psi_1\gamma^2 = P_{yy} - P_{xx}$ and $\psi_2\gamma^2 = P_{zz} - P_{yy}$. Both material functions for all liquid pentane isomers at 273.15 K are well described by the γ power law for the range of shear rate in this study. The signs of the material functions for normal pentane and isopentane are consistent with the experimental shear flow, that is $\psi_1 > 0$ and $\psi_2 < 0$, but both are negative for neopentane. The ratio ψ_2/ψ_1 is different for all liquid pentane isomers. It is -0.87 for normal pentane, -1.77 for isopentane, and 1.79 for neopentane. The experiment gives values of ≥ -0.4 [40]. Another useful quantities derived from normal stress differences are the out-of-plane and

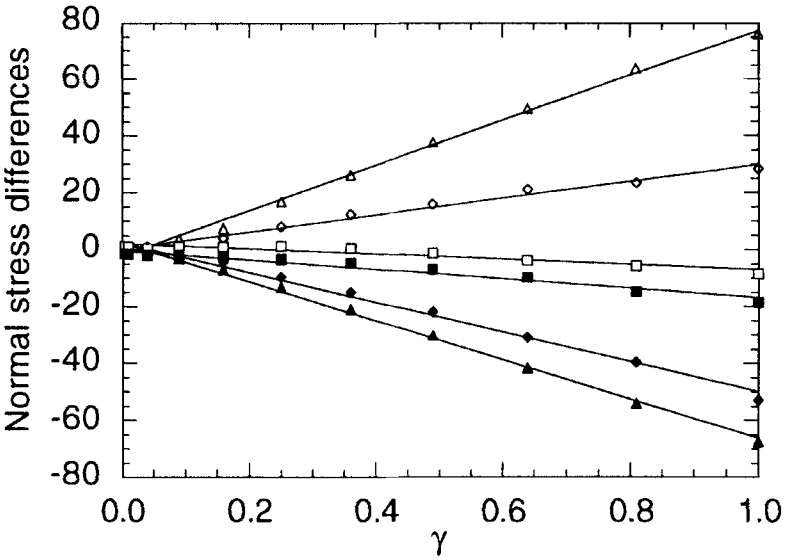

FIGURE 4 The strain rate dependent normal stress difference(MPa) at 273.15 K. Open ones: $\langle p_{yy} - p_{xx} \rangle$ and filled ones: $\langle p_{zz} - p_{yy} \rangle$.

in-plane normal stress coefficients, η_0 and η_-, defined as $2\gamma\eta_0 = (P_{xx} + P_{yy})/2 - P_{zz}$ and $2\gamma\eta_- = P_{yy} - P_{xx}$ [41]. We see that the in-plane normal stress coefficients for all liquid pentane isomers are constant for the range of shear rate in this study and are 79.4, 29.6, and -9.29 MPa · ps, respectively.

In Figures 5 and 6, we plot the strain rate dependent mean square of the radius of gyration and average end-to-end distance for normal pentane and

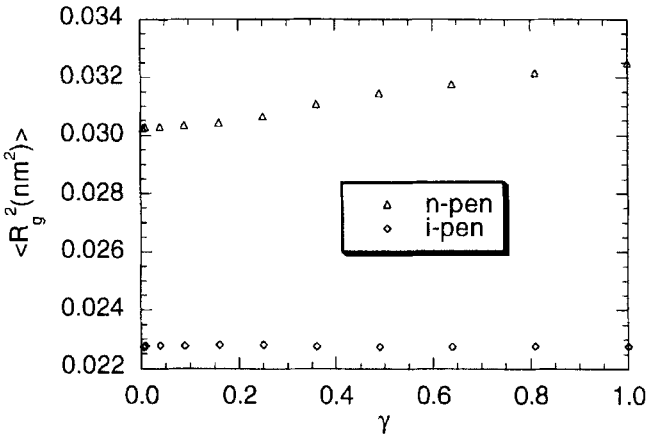

FIGURE 5 The strain rate dependent square of radius of gyration of the expanded collapsed atom model for liquid pentane isomers at 273.15 K.

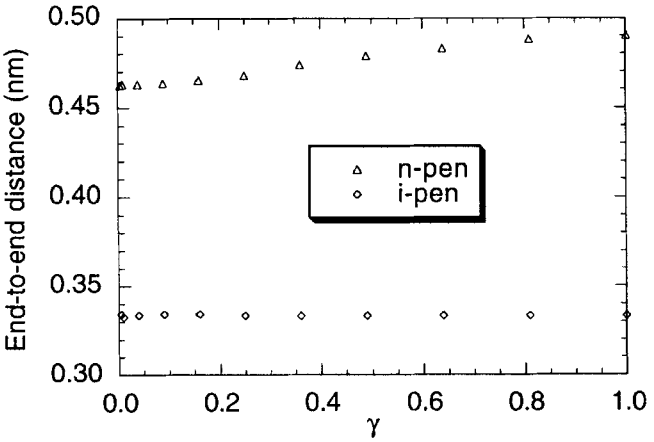

FIGURE 6 The strain rate dependent average end-to-end distance of the expanded collapsed atom model for liquid pentane isomers at 273.15 K.

isopentane at 273.15 K. The equilibrium values of R_g^2 and end-to-end distance are 0.0302 nm^2 and 0.462 nm for normal pentane, and 0.0226 nm^2 and 0.332 nm for isopentane. As can be seen from the figures, the overall trend of the square of radius of gyration and end-to-end distance for normal pentane is a linear increase with strain rate. But for isopentane, the values are virtually changed for the range of shear rate in this study. The variation for normal pentane with the strain rate shows two different slopes – almost zero dependent at very low strain rate ($< 0.09\,\text{ps}^{-1}$) and a linear increase with the strain rate at a relatively high strain rate greater than $0.16\,\text{ps}^{-1}$, reflecting the fact that the molecules are under various conformations with different percentages of C—C—C—C *trans*, as shown in Figure 7, and with shear induced stretching and bending. On the other hand, for isopentane, the variation of R_g^2 and end-to-end distance with strain rate is very small for the range of shear rate studied, not much different from the equilibrium value. This reflects that the chain is very stiff for such branched-chain alkanes for the range of strain rate.

Figure 7 shows the strain rate dependent alignment angle for normal pentane and isopentane and the average percentage of C—C—C—C *trans* for normal pentane at 273.15 K. The alignment angle is simply defined by

$$\alpha = \tan^{-1}(\langle y \rangle / \langle x \rangle), \tag{13}$$

where $\langle x \rangle$ and $\langle y \rangle$ are the x- and y-components of the average end-to-end distance. The equilibrium value of the alignment angle at the zero strain rate

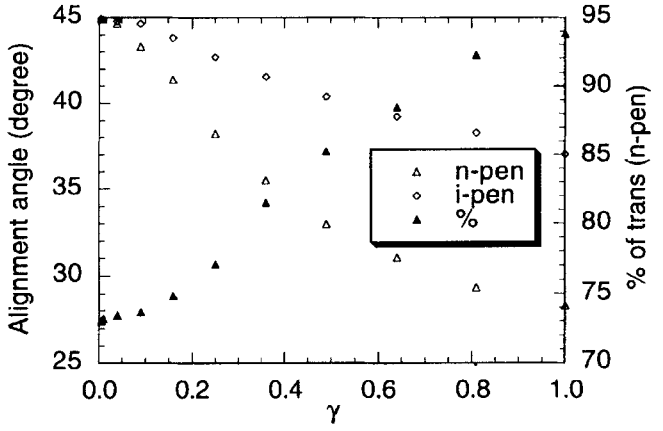

FIGURE 7 The strain rate dependent alignment angle defined Eq. (13) and percentage of C—C—C—C *trans* of the expanded collapsed atom model for liquid pentane isomers at 273.15 K.

reaches 45°, consistent with other NEMD studies for decane, hexadecane, and tetracosane [38]. The general trend is that the alignment angle decreases with increasing strain rate and the alignment angle of the straight chain alkane is less than that of the branched chain alkane. The straight chain alkane molecules slide past each other with the same viscosity as the branched chain alkane molecules by aligning themselves better. Because of a doubly imposed torsional rotational potential on the 2–3 bond in isopentane as shown Figure 1, the dihedral states of 1–2–3–4 and 5–2–3–4 are nearly fixed. The average percentage of C—C—C—C *trans* is related to the doubly imposed dihedral state in such a way that if the dihedral state of 1–2–3–4 is in *trans*, then the dihedral state of 5–2–3–4 must be in *gauche*, or *vice versa*. For normal pentane, the average percentage of C—C—C—C *trans* as a function of strain rate is in excellent correlation with the square of radius of gyration and the average end-to-end distance as seen in Figures 5 and 6. At low strain rate ($< 0.09\,ps^{-1}$), the percentage of *trans* increases very slowly with increasing strain rate and shows a sharp linear increase with strain rate at high strain rate. Applying the strain rate in the x-direction, the alignment angle is forced to decrease and the percentage of C—C—C—C *trans* to increase with increasing strain rate.

IV. CONCLUSION

In this paper, we have presented NEMD simulations of the expanded collapsed atom model for liquid pentane isomers at 273.15 K. It is found that the strain rate dependent viscosities for liquid pentane isomers exhibit a shear-thinning and a linear dependence on $\gamma^{1/2}$, and that the Newtonian viscosities for liquid pentane isomers obtained by a linear extrapolation to zero strain rate are: 0.256 cP for normal pentane, 0.219 cP for isopentane, and 0.168 cP for neopentane. This reflects the fact that as the molecular shape tends to approach that of a sphere and the surface area tends to decrease with branching, the viscosity of liquid pentane isomers decreases.

Acknowledgments

This research was supported by the Basic Science Research Institute Program, Ministry of Education (BSRI-98-3414). The author thanks the Computer Center at Electronics and Telecommunications Research Institute for access to its Cray-C90 super computer and the Tongmyung University of Information Technology (Pusan. Korea) for access to its IBM SP/2 computers.

References

[1] Solomon, T. W. G. (1988). Organic Chemistry, 4th edn. (John Wiley and Sons, New York).

[2] Diller, D. E. and van Poolen, L. J. (1985). "Measurements of the viscosities of saturated and compressed liquid normal butane and isobutane", *Int. J. Thermophysics.*, **6**, 43.

[3] Weast, R. C. and Astle, M. J. (1982–1983). CRC Handbook of Chemistry and Physics (CRC press, Boca Ranton), 63rd edn.

[4] Chynoweth, S., Klomp, U. C. and Michopoulos, Y. (1991). "Comment on: Rheology of *n*-alkanes by nonequilibrium molecular dynamics", *J. Chem. Phys.*, **95**, 3024.

[5] Chynoweth, S., Klomp, U. C. and Scales, L. E. (1991). "Simulation of organic liquids using pseudo-pairwise interatomic forces on a toroidal transputer array", *Comput. Phys. Commun.*, **62**, 297.

[6] Berker, A., Chynoweth, S., Klomp, U. C. and Michopoulos, Y. (1992). "Non-equilibrium molecular dynamics (NEMD) simulations and the rheology properties of liquid *n*-hexadecane", *J. Chem. Soc. Faraday Trans.*, **88**, 1719.

[7] Ryckaert, J. P. and Bellemans, A. (1978). "Molecular dynamics of liquid alkanes", *Discuss. Faraday Soc.*, **66**, 95.

[8] Lee, S. H. and Cummings, P. T. (1996). "The rheology of *n*-butane and *i*-butane by non-equilibrium molecular dynamics simulations", *Mol. Sim.*, **16**, 229.

[9] Lee, S. H. and Cummings, P. T. (1998). "The rheology of *n*-decane and 4-propyl heptane by non-equilibrium molecular dynamics simulations", *Mol. Sim.*, **21**, 27.

[10] Lee, S. H. (1999). "The rheology of 6-propyl duodecane and 5-dibutyl nonane by non-equilibrium molecular dynamics simulations", *Mol. Sim.*, in press.

[11] Lee, S. H., Lee, H., Pak, H. and Rasaiah, J. C. (1996). "Molecular dynamics simulation of liquid alkanes. I. Thermodynamics and structures of normal alkanes: *n*-butane to *n*-heptadecane", *Bull. Kor. Chem. Soc.*, **17**, 735.

[12] Lee, S. H., Lee, H. and Pak, H. (1997). "Molecular dynamics simulation of liquid alkanes. II. Dynamic properties of normal alkanes: *n*-butane to *n*-heptadecane", *Bull. Kor. Chem. Soc.*, **18**, 478.

[13] Lee, S. H., Lee, H. and Pak, H. (1997). "Molecular dynamics simulation of liquid alkanes. III. Thermodynamic, structural, and dynamic properties of branched-chain alkanes", *Bull. Kor. Chem. Soc.*, **18**, 501.

[14] White, D. N. J. and Boville, M. J. (1977). "Molecular mechanics calculations on alkanes and non-conjugated alkanes", *J. Chem. Soc. Perkin Trans.*, **2**, 1610.

[15] Davis, P. J. and Evans, D. J. (1994). "Comparison of constant pressure and constant volume nonequilibrium simulations of sheared model decane", *J. Chem. Phys.*, **100**, 541.

[16] Evans, D. J. and Morriss, G. P. (1990). Statistical Mechanics of Nonequilibrium Liquids (Academic: New York).

[17] deGroot, S. R. and Mazur, P. (1984). Non-equilibrium Thermodynamics (Dover: New York).

[18] Evans, D. J. and Morriss, P. (1984). "Nonlinear response theory for steady planar Couette flow", *Phys. Rev. A*, **30**, 1528.

[19] Evans, D. J. and Morriss, P. (1984). "Non-Newtonian molecular dynamics", *Comput. Phys. Repts.*, **1**, 297.

[20] Lees, A. W. and Edwards, S. F. (1972). "The computer study of transport processes under extreme conditions", *J. Phys. C: Solid State*, **5**, 1921.

[21] Muller-Plathe, F., Rogers, S. C. and van Gunsteren, W. F. (1993). "Gas sorption and transport in polyisobutylene: Equilibrium and nonequilibrium molecular dynamics simulations", *J. Chem. Phys.*, **98**, 9895.

[22] Evans, D. J., Hoover, W. G., Failor, B. H., Moran, B. and Ladd, A. J. C. (1983). "Nonequilibrium molecular dynamics via Gauss's principle of least constraint", *Phys. Rev. A*, **28**, 1016.

[23] Simmons, A. D. and Cummings, P. T. (1986). "Non-equilibrium molecular dynamics simulation of dense fluid methane", *Chem. Phys. Lett.*, **129**, 92.

[24] Gear, C. W. (1971). Numerical Initial Value Problems in Ordinary Differential Equation (Prentice-Hall, Englewood Cliffs, NJ).

[25] Lee, S. K. and Lee, S. H. (1999). "Molecular dynamics simulation studies of physico chemical properties of liquid pentane isomers", *Bull. Kor. Chem. Soc.*, **18**, in press.
[26] Yamada, T. and Kawasaki, K. (1975). "Application of mode-coupling theory to nonlinear stress tensor in fluids", *Prog. Theor. Phys.*, **53**, 111.
[27] Kawasaki, K. and Gunton, J. D. (1973). "Theory of nonlinear transport processes: Nonlinear shear viscosity and normal stress effects", *Phys. Rev. A*, **8**, 2048.
[28] Ernst, M. H., Cichocki, B., Dorfman, J. R., Sharma, J. and van Beijeren, H. J. (1978). "Kinetic theory of nonlinear viscous flow in two and three dimensions", *J. Stat. Phys.*, **18**, 237.
[29] Lee, S. H. and Cummings, P. T. (1993). "Shear viscosity of model mixtures by non-equilibrium molecular dynamics. I. Argon-krypton mixtures", *J. Chem. Phys.*, **99**, 3919.
[30] Lee, S. H. and Cummings, P. T. (1994). "Effect of three-body forces on the shear viscosity of liquid argon", *J. Chem. Phys.*, **101**, 6206.
[31] Lee, S. H. and Cummings, P. T. (1996). "Shear viscosity of model mixtures by nonequilibrium molecular dynamics. II. Effect of dipolar interactions", *J. Chem. Phys.*, **105**, 2044.
[32] Cummings, P. T. and Evans, D. J. (1992). "Nonequilibrium molecular dynamics approaches to transport properties and non-Newtonian fluid rheology", *Ind. Eng. Chem. Res.*, **31**, 1237.
[33] Edberg, R., Morriss, G. P. and Evans, D. J. (1987). "Rheology of *n*-alkanes by nonequilibrium molecular dynamics", *J. Chem. Phys.*, **86**, 4555.
[34] Morriss, G. P., Daivis, P. J. and Evans, D. J. (1991). "The rheology of *n*-alkanes: Decane and eicosane", *J. Chem. Phys.*, **94**, 7420.
[35] Daivis, P. J., Evans, D. J. and Morriss, G. P. (1992). "Computer simulation study of the comparative rheology of branched and linear alkanes", *J. Chem. Phys.*, **97**, 616.
[36] Rowley, R. L. and Ely, J. F. (1991). "Non-equilibrium molecular dynamics simulations of structured molecules: Part I. Isomeric effects on the viscosity of butnaes", *Mol. Phys.*, **72**, 831.
[37] Cui, S. T., Cummings, P. T. and Cochran, H. D. (1996). "Multiple time step non-equilibrium molecular dynamics simulation of the rheological properties of liquid *n*-decane", *J. Chem. Phys.*, **104**, 255.
[38] Cui, S. T., Gupta, S. A., Cummings, P. T. and Cochran, H. D. (1996). "Molecular dynamic simulationjs of the rheology of normal decane, hexadecane, and tetracosane", *J. Chem. Phys.*, **105**, 1214.
[39] Clarke, J. H. and Brown, D. (1987). "The rheological properties of liquids composed of flexible chain molecules: a molecular dynamics simulation study", *J. Chem. Phys.*, **86**, 1542.
[40] Bird, R. B., Hassager, O., Amstrong, R. C. and Curtiss, C. F. (1977). Dynamics of Polymeric Liquids Vol. 1: Fluid Mechanics 2nd edn. (Wiley, New York); Bird, R. B., Hassager, O., Amstrong, R. C. and Curtiss, C. F. (1977). Dynamics of Polymeric Liquids Vol. 2: Kinetic Theory 2nd edn. (Wiley, New York).
[41] Hess, S. (1983). "Similarities and differences in the nonlinear flow behavior of simple and molecular liquids", *Physica A*, **118**, 79.